INTERNATIONAL JOURNAL OF HYDROGEN ENERGY 40 (2015) 735–745

Available online at www.sciencedirect.com

ScienceDirect

journal homepage: www.elsevier.com/locate/he

CFD analysis of fast filling strategies for hydrogen tanks and their effects on key-parameters

*Daniele Melideo, Daniele Baraldi**

European Commission DG-Joint Research Centre (JRC), Institute for Energy and Transport, P.O. Box 2, 1755 ZG, Petten, The Netherlands

ARTICLE INFO

Article history:
Received 23 June 2014
Received in revised form
14 October 2014
Accepted 30 October 2014
Available online 29 November 2014

Keywords:
Fast filling
Compressed hydrogen storage
CFD
Hydrogen safety
State of charge

ABSTRACT

A major requirement for the filling of hydrogen tanks is the maximum gas temperature within the vessels during the process. Different filling strategies in terms of pressure and temperature of the gas injected into the cylinder and their effects on key parameters like maximum temperature, state of charge, and energy cooling demand are investigated. It is shown that pre-cooling of the gas is required but is not necessary for the whole duration of the filling. Relevant energy savings can be achieved with pre-cooling over a fraction of the time. The most convenient filling strategy from the cooling energy point of view is identified: with an almost linear pressure rise and pre-cooling in the second half of the process, a 60% reduction of the cooling energy demand is achieved compared to the case of pre-cooling for the whole filling.

Introduction

The deployment of hydrogen powered vehicles requires a distributed network of hydrogen refuelling stations and the definition of the filling protocols for hydrogen tanks. With conventional fuel powered vehicles, drivers are used to refill the tank in few minutes and they expect to spend the same time for a new technology like hydrogen cars. The combination of the need for similar driving range between conventional fuel and hydrogen vehicles with the very low density of hydrogen brings the necessity to fill the hydrogen tanks to very high pressure (i.e. up to 70 MPa). Filling the tank in a short time (~3 min) at high pressure creates some issues. The rapid compression generates an increase of gas temperature inside the vessel and because of heat transfer the temperature of the tank material increases with time. If the temperature augments too much, the structural integrity of the tank might be jeopardized. Because of safety, the maximum allowed temperature inside tanks is set to 85 °C (358 K) by the majority of the international standards and regulations (e.g. the European regulation [1], the SAE [2,3], the global technical regulation [4], and the international standard ISO 15869 [5]). Beyond the safety considerations, the increase of temperature has a negative consequence on the gas density and subsequently on the total amount of gas that is injected in the tank during the filling. The state of charge (SOC) is defined as the ratio (in percentage) between the density at the end of the filling process and the density at 70 MPa and 15 °C or at 87.5 MPa and 85 °C (40.2 kg/m^3). The SOC gives an indication of the filling degree and it is strictly related to the temperature and pressure. A high value very close to 100% is desirable because it

* *Corresponding author.*
E-mail address: daniele.baraldi@ec.europa.eu (D. Baraldi).
http://dx.doi.org/10.1016/j.ijhydene.2014.10.138

provides a larger driving range. At the same time, the SOC should not exceed 100% as it is described in the operating conditions of the vehicle fuel system [2,3]. It has been shown both experimentally and by numerical simulations that the temperature threshold can be exceeded e.g. a 29 L tank type 4 that is refilled in 200 s at 20 °C of ambient temperature [6,7]. The technological solution envisaged to tackle that issue is to pre-cool the gas before injecting it into the tank. However the addition of the heat exchanger to the refuelling installation causes a significant increase in the initial cost of the station and in the running costs in terms of energy consumption. Reducing the cooling demand has a positive effect on the energy consumption (and the running costs) and therefore on all the environmental parameters that are related to the energy consumption e.g. pollution emissions and greenhouse gas emissions in the case of electricity from fossil fuel plants.

Two key parameters to control the filling process are the temperature and pressure profile of the gas which flows in the vessel. The main objective of the paper is to assess the effect of different filling strategies on the maximum gas temperature at the end of the process, on the SOC and on the cooling demand. It must be emphasized that the aim of the paper is not optimization, e.g. to define the optimum strategy for the filling, but to investigate the effects of different filling approaches on those key-parameters and to identify tendencies that can help to define suitable filling strategies.

The analysis is based on CFD calculations. It must be highlighted that the accuracy of the applied CFD model was successfully assessed by comparison with experimental data at different experimental conditions [7–10]. The great interest in CFD modelling as an analysis and investigation tool for hydrogen fast filling issues has been demonstrated by the increasing number of publications in the field in the last decade [11–19].

Four series of simulations have been performed with different strategies for the profiles of pressure and temperature of the incoming gas as described in Table 1. Initially we have considered an almost linear pressure rise with constant temperature (cases 1). As a second step, we have selected a step-wise pressure rise with constant temperature (cases 2). Third, we have imposed a step-wise temperature profile with the almost linear pressure profile (cases 3). Finally we have selected a step-wise function both for the pressure rise and for the temperature profile (cases 4).

Table 1 – Parameters of the investigated cases.

Case	Scenario	T	Initial time of cooling	Duration of the cooling	P
1A	Constant T	15 °C	–	–	Ref
1B	Constant T	0 °C	0 s	204 s	Ref
1C	Constant T	−20 °C	0 s	204 s	Ref
1D	Constant T	−40 °C	0 s	204 s	Ref
2A	Varying P	15 °C	–	–	/‾
2B	Varying P	15 °C	–	–	_/
2C	Varying P	15 °C	–	–	Step
2A_pre	Varying P	−40 °C	0 s	204 s	/‾
2B_pre	Varying P	−40 °C	0 s	204 s	_/
2C_pre	Varying P	−40 °C	0 s	204 s	Step
3A	Increasing T	_/‾	0 s	30 s	Ref
3B	Increasing T	_/‾	0 s	50 s	Ref
3C	Increasing T	_/‾	0 s	120 s	Ref
3D	Decreasing T	‾_	100 s	104 s	Ref
4A	Combined	‾_	100 s	104 s	_/
4B	Combined	_/‾	0 s	170 s	_/
4C	Combined	‾_	40 s	164 s	/‾
4D	Combined	_/‾	0 s	120 s	/‾
4E	Combined	‾_	50 s	154 s	Step
4F	Combined	_/‾	0 s	120 s	Step

CFD model set-up

The CFD model set-up was based on the modelling strategy that was successfully adopted in the validation investigation [7–10]. The numerical simulations have been performed with the commercial CFD software ANSYS CFX V14.0 [20]. In CFX a conjugate heat transfer model is available (CHT) with the capability of capturing the thermal conduction through solid materials coupled with the changing temperature in the fluid. The numerical time scheme is based on a Second Order Backward Euler scheme. The high resolution scheme of CFX has been selected for the advection terms. Further details on the numerical scheme can be found in the ANSYS CFX manual [20]. A residual convergence criterion for RMS (root mean square) mass-momentum equations of 10^{-4} has been applied, ensuring the attainment of convergence of results.

Since at high pressure the ideal gas law is not accurate enough to describe the pressure and temperature behaviour [8], a real gas equation of state for the evaluation of hydrogen properties has been used (Redliche–Kwong [21]). A modified k–ε approach [22] was applied as turbulence model in order to reduce the jets spreading rate over-prediction of the standard model [22–24]. In the modified model, the value of the

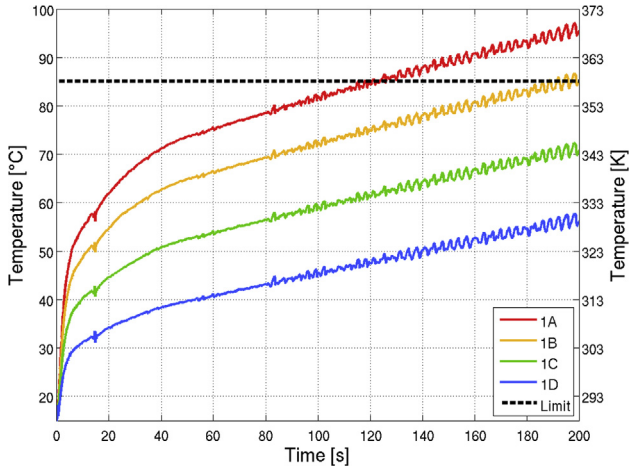

Fig. 1 – Temperature history for cases 1A ($T = 15$ °C), 1B ($T = 0$ °C), 1C ($T = -20$ °C), and 1D ($T = -40$ °C).

constant coefficient, Cε1, of the production term in the dissipation equation was increased from 1.44 to 1.52 [22]. At every fluid–solid interface a no-slip boundary condition was applied. More details on the CFD modelling strategy can be found in a series of papers by the same group of authors [7–10].

Initial configuration

The initial configuration for this study was selected because it was already investigated from the experimental point of view [6] and subsequently from the numerical point of view [9]. The experiments were carried out in the JRC experimental facility GasTeF [6]. Those experiments were used for the validation of the same CFD model that is applied for the simulations in this paper. Several validation studies have been performed in recent years with the same CFD model [7–10].

A type IV tank was selected for the investigation because the temperature rise is usually larger in a type 4 than in a type 3 tank for the same initial and boundary conditions during the filling. The main difference between the tanks is that a type 4 tank has a plastic liner while in type 3 the liner is metallic. The larger temperature increase is due to the different thermal insulation properties of the plastic material compared to the metallic one. In the type 3 tank the heat transfer from the gas to the external environment through the tank walls is faster, causing a smaller temperature rise inside the tank compared to the type 4 tank.

The volume of the tank is 28.9 L and the initial vessel pressure is equal to 2 MPa which corresponds to an almost empty tank (~50 g of hydrogen that are sufficient for a 5 km trip). The final pressure is 77.5 MPa and the filling time is 204 s. Those initial and final conditions, and the gas inlet pressure history were selected from one of the experiments that was used for validation purposes [6,9]. The final pressure is higher than 70 MPa since the final temperature at the end of the filling is higher than the ambient temperature because of the compression. After the end of the filling, the heat transfer between the tank and the environment continues until the tank temperature equals the ambient temperature, with the effect of decreasing the temperature and pressure of the vessels. Therefore the final pressure of the filling must be higher than 70 MPa in order to have 70 MPa and the desired density (40.2 kg/m^3) at the ambient temperature. For the specific tank size (28.9 L) in this investigation, the 100% SOC is reached when the total mass inside the vessel is 1.16 kg.

For this type of tank, it has been shown both experimentally and numerically that the temperature can be considered as uniform in the tank apart from some small regions [6,9]. The incoming jet is colder than the gas inside the vessel and therefore it generates a temperature gradient in a relatively thin region along the tank centreline until a distance where the incoming gas is well mixed with the gas inside the tank. Another temperature gradient can be found in the regions near to the tank walls e.g. in the thermal boundary layer formed by heat transfer from the gas to the tank walls. Since the temperature can be considered uniform during the filling apart from limited regions which contribute with a negligible impact to the calculation of the averaged gas temperature in the vessel, the results of the calculations are shown for only one position in the upper part of the tank in the middle section which is representative of the gas temperature history in the whole tank.

The theoretical cooling demand of the heat exchanger without considering any losses has been calculated as:

$$Q = \dot{m}(h_{in} - h_{out}). \quad (1)$$

where $\dot{m}$ is the mass flow rate, h_{in} and h_{out} are the enthalpies of the gas which is going in and out of the heat exchanger respectively. The total energy cooling demand is calculated as a time integral of the above expression.

Results and discussion

Linear pressure rise and constant temperature profile – cases 1

In Fig. 1 temperature histories with no-pre-cooling (case 1A with $T = 15$ °C), and 3 levels of pre-cooling (case 1B with $T = 0$ °C, case 1C with $T = -20$ °C, and case 1D with $T = -40$ °C) are shown. The selection of the 4 cases 1 has been made according to the SAE J2601 where 4 different pre-cooling possibilities are foreseen: no-precooling, 0 °C, −20 °C, and −40 °C. In Fig. 1 it is demonstrated that pre-cooling is required to keep the maximum temperature below the limit. If the gas is pre-cooled to −40 °C and to −20 °C, the maximum temperature at the end of the filling is below the 85 °C threshold. With the milder pre-cooling to 0 °C, the maximum temperature is at the threshold while with no pre-cooling, the temperature is above the limit by about 10°. In all cases the steeper temperature increase occurs in the first 20 s when the mass flow rate increases to its maximum value. The pressure profile is almost linear and it is depicted in red (in the web version) colour in Fig. 2 (left-hand side). That pressure profile will be identified as the reference pressure profile in the paper and in the legends.

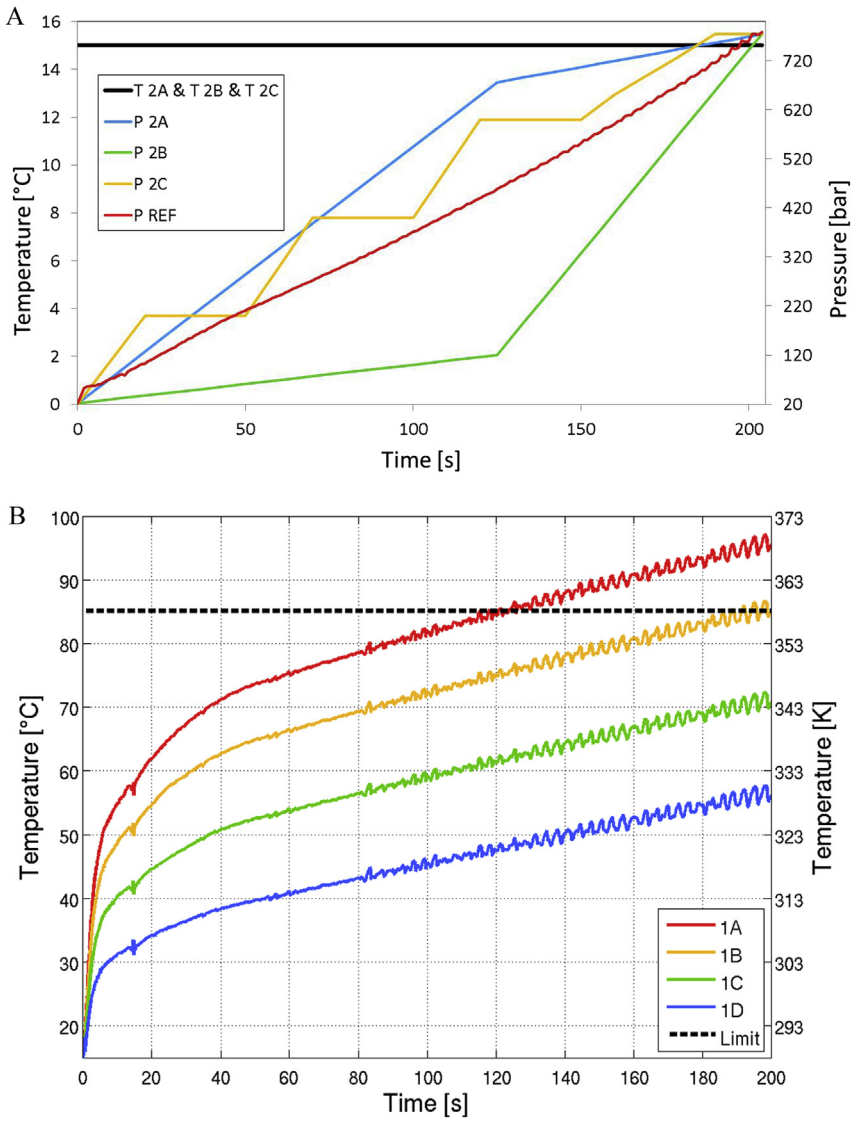

Fig. 2 – Left-hand side: pressure and temperature history of the gas entering the tank for cases 1A, 2A, 2B, and 2C (no-precooling). Right hand side: temperature history of the gas inside the tank for cases 2A, 2B and 2C.

Step-wise pressure rise and constant temperature profile (no pre-cooling) – cases 2

To evaluate the effects of the pressure history, different pressure profiles have been applied to the gas entering into the tank at a constant temperature of 15 °C, as illustrated in Fig. 2 (left-hand side). Compared to the reference pressure profile that has an almost linear behaviour, three different step-wise profiles have been considered: a profile with faster initial pressure rise and slower final pressure rise (case 2A – decreasing pressure rise rate), a profile with slower initial pressure rise and faster final pressure rise (case 2B – increasing pressure rise rate), and a profile with multiple steps (case 2C). As shown in Fig. 2 (right-hand side) modifying the pressure profile causes a significant difference in the gas temperature history and in the maximum temperature but for none of the profiles the final temperature is lower than the threshold value. The strategy of step-wise pressure rise is not successful and pre-cooling is needed. That conclusion is consistent with the experimental findings in the research of Hirotani and co-workers [25].

In Figs. 1 and 2 (right-hand side) after the initial filling stages, fluctuations appear in the temperature history for case 1A which is the case that reproduces the experiment. The reason can be found in the pressure history of the incoming gas. In the experiments the filling of the tank occurs directly from a high pressure reservoir in the initial stages of filling while in the following stages a compressor increases the pressure of the gas coming from the reservoir before injecting the gas into the tank. The fluctuations in the pressure of the incoming gas are produced by the motion of the piston of the compressor. Those pressure fluctuations generate the small oscillations in the temperature history both in the experiment and in the simulations when the same pressure profile is employed at the inlet pipe as boundary condition for the incoming gas. We have kept the experimental pressure

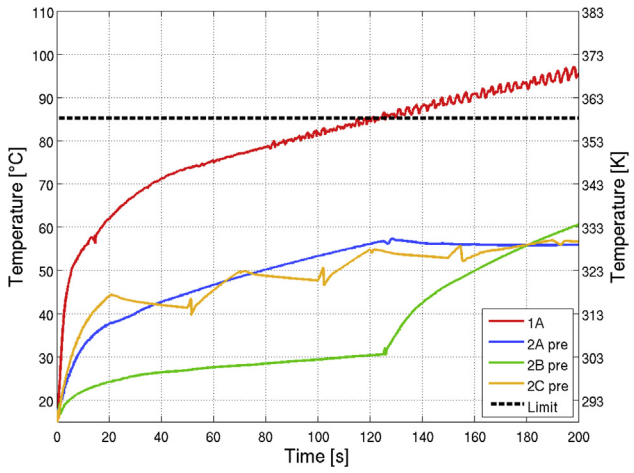

Fig. 3 – Temperature history of the gas inside the tank for cases 2A_pre, 2B_pre and 2C_pre (with pre-cooling).

history, including the fluctuations, for each case except when investigating variations from the reference incoming pressure profile like in the cases 2B, 2C and 2D. In those cases, we have generated new pressure profiles to investigate the effect of different pressure rises on the gas temperature history. Since those fluctuations do not affect the behaviour of the parameters that are investigated in this work, they have not been included in the generated pressure profiles.

When pre-cooling to −40 °C is applied for the whole duration of the process to the pressure profiles that are illustrated in Fig. 2 (left-hand side), the maximum temperature stays below the threshold for all three cases (case 2A_pre, case 2B_pre, and case 2C_pre) as shown in Fig. 3. The maximum temperatures of all cases 2_pre are in a similar range (55–60 °C) as for case 1D (55 °C). The total cooling energy demand is also similar (the cooling demand of each case is listed in Table 2): for case 1D is 874 KJ while for case 2A_pre, case 2B_pre, and case 2C_pre it is 880 KJ, 829 KJ, and 882 KJ respectively. In case 2B_pre it is possible to save 5% of cooling energy compared to case 1D, while case 2A_pre and case 2C_pre are slightly more energy consuming.

From the point of view of the maximum temperature, the worst strategies for the pressure profile are the case 2B in the right-hand side of Fig. 2 and case 2B_pre in Fig. 3 where the pressure rise is slow in the first half of the filling and it is fast in the second half. In cases 2A and 2A_pre, the slow pressure rise in the second half produces a decrease of temperature. A decrease of temperature occurs also in cases 2C and 2C_pre in those time periods where the pressure of the incoming gas is kept constant. During those times, the increase of pressure and temperature due to the incoming gas is absent and because of the heat transfer to the tank walls, the gas temperature decreases. The non-monotonic behaviour in the temperature history in cases 2A and 2C is caused by the decrease in the pressure profile of the incoming gas.

Linear pressure rise and step-wise temperature profile – cases 3

To investigate whether pre-cooling is required for the whole duration of the filling, four pre-cooling strategies are considered as shown in Fig. 4 (left-hand side): the gas is pre-cooled to −40 °C only for the first 10 s (case 3A), for the first 30 s (case 3B), for the first 100 s (case 3C), and for the last 100 s (case 3D). The effect of the cooling is clearly visible in Fig. 4 (right-hand side). In cases 3A and 3B, as soon as the precooling of the gas is stopped, the gas temperature inside the tank increases quickly and the final temperature exceeds the allowed maximum value. Extending the pre-cooling to the first 100 s in case 3C is sufficient to limit the maximum temperature with a final temperature that is equal to 75 °C. A similar final temperature (78 °C) is reached if the gas is pre-cooled in the last 100 s (case 3D) while the maximum temperature is about 83 °C. Case 3D is the only case with the reference pressure profile where the gas temperature does not increase monotonically.

In Fig. 4 it is demonstrated that pre-cooling to −40 °C for the whole duration of the filling is not necessary and that pre-cooling for half of the time is sufficient with a significant saving in cooling energy. In cases 3C and 3D, the energy saving is 36.5% and 60% respectively compared to case 1D as shown in Table 2. Case 1D is the case where the cooling to −40 °C is applied for the whole duration of the filling and it is the most

Table 2 – Relevant data for all cases with maximum temperature below the threshold of 85 °C. The energy savings are calculated with case 1D as a reference case.

Case	Total cooling demand [kJ]	Energy saving [%]	Max cooling demand [kW]	Total Mass [kg]	S.O.C. [%]	Max temp reached [°C]
1C	537.8	−38.49	~6	1.1047	95.10	70
1D	874.3	–	~10	1.1387	98.02	55
2A_pre	880.8	0.74	~10	1.1357	97.76	55
2B_pre	829.4	−5.14	~13	1.0973	94.44	55
2C_pre	882.8	0.97	~18	1.1406	98.17	60
3C	540.0	−38.23	~10	1.0968	94.40	74
3D	346.5	−60.37	~5	1.0382	89.36	83
4A	705.2	−19.34	~15	1.0601	91.25	65
4B	520.4	−40.48	~13	1.0844	93.34	78
4C	502.4	−42.54	~7	1.1078	95.35391	82
4D	722.7	−17.34	~13	1.0748	92.51	65
4E	484.5	−44.58	~12	1.1073	95.31397	85
4F	606.5	−30.63	~10	1.10622	95.22	70

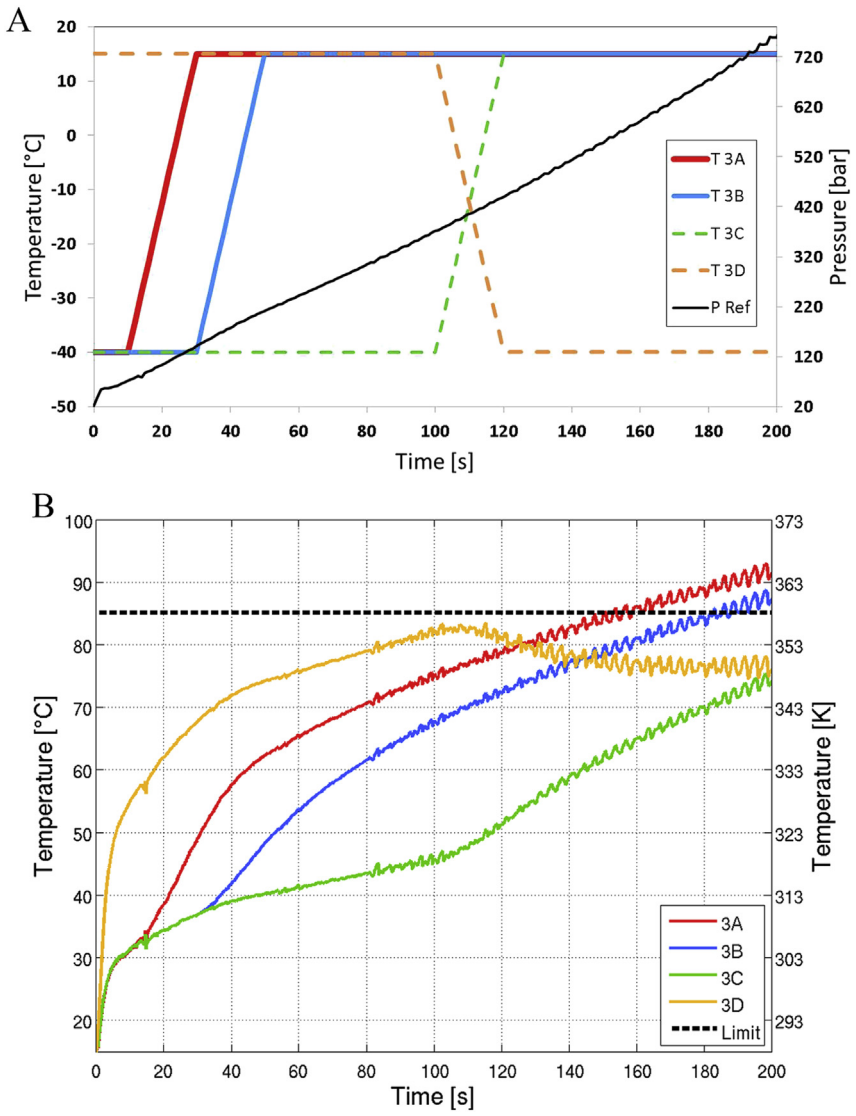

Fig. 4 – Left-hand side: pressure and temperature history of the gas entering the tank for cases 3A, 3B, 3C, and 3D. Right-hand side: Temperature history of the gas inside the tank for cases 3A, 3B, 3C, and 3D.

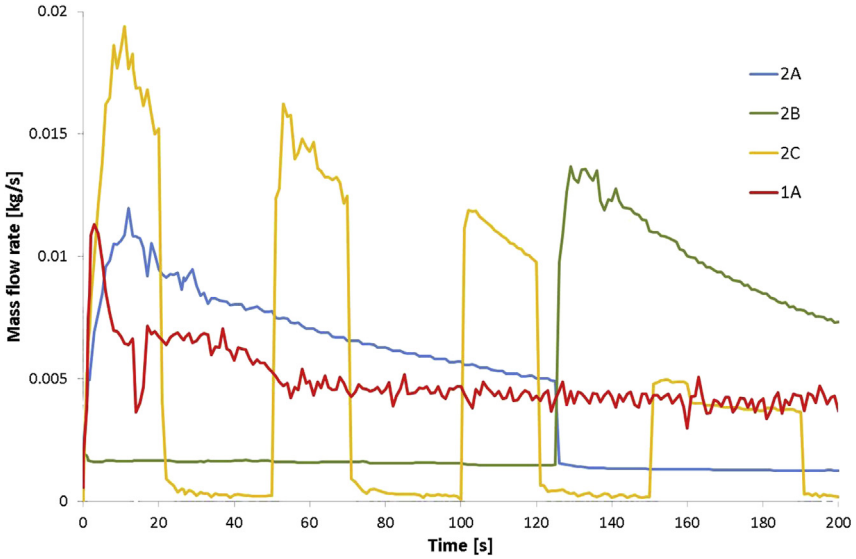

Fig. 5 – Mass flow rate history for cases 1A, 2A, 2B, and 2C.

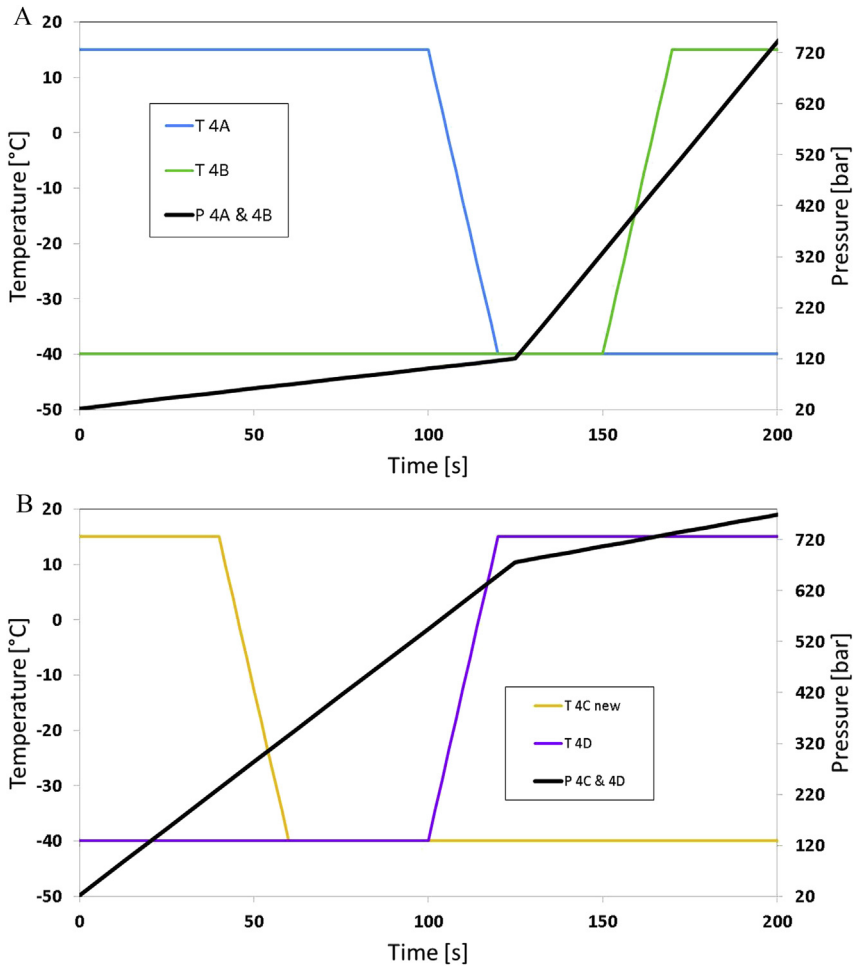

Fig. 6 – Left-hand side: pressure and temperature history of the gas entering the tank for cases 4A and 4B. Right-hand side: pressure and temperature history of the gas entering the tank for cases 4C and 4D.

demanding case from the cooling energy point of view with case 2A_pre and case 2C_pre.

Cooling the gas in the second half of the filling is more efficient than in the first half from the point of view of the cooling energy since the mass flow rate in the second half is lower than in the first half as shown in Fig. 5 for the case 1A without cooling.

One of the relevant parameters that affects the temperature increase within the tank is the mass filling rate that depends mainly on the pressure ratio between the hydrogen reservoir (or compressor) and the tank pressure. In Fig. 5 the mass flow rate histories for the cases 1A, 2A, 2B, and 2C are illustrated. The mass flow rate is a relevant parameter for the calculation of the cooling energy as shown in equation (1). For the same temperature difference of the gas at the inlet and outlet of the heat exchanger, the cooling energy demand depends on the mass flow rate. The large fluctuations in the 1A profile have been filtered in order to make the figure more easily readable.

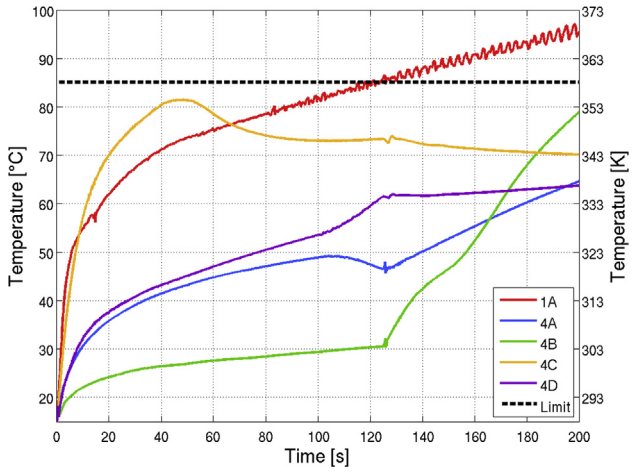

Fig. 7 – Temperature history of the gas inside the tank for cases 4A, 4B, 4C, and 4D.

Step-wise pressure rise and step-wise temperature profile – cases 4

Finally step-wise functions have been considered both for the pressure and temperature profiles of the incoming gas as shown in Table 1. The same pressure profile of case 2B in Fig. 2 without pre-cooling is applied to cases 4A and 4B with pre-

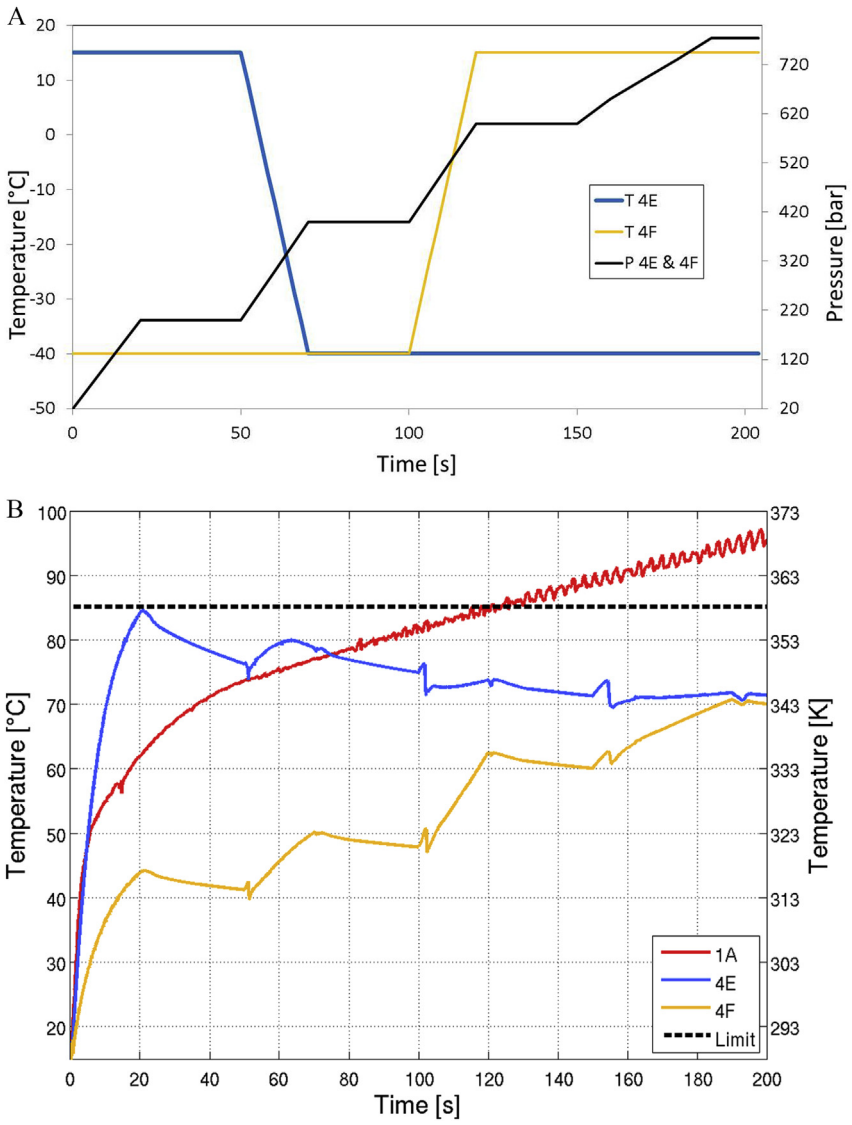

Fig. 8 – Left-hand side: pressure and temperature history of the gas entering the tank for cases 4E and 4F. Right-hand side: temperature history of the gas inside the tank for cases 4E and 4F.

cooling. The case 2B (two-step pressure rise with increasing rise rate) is a particularly critical case since the maximum temperature without pre-cooling is the largest one as illustrated in Fig. 2 (right-hand-side). When pre-cooling is applied for the last 100 s (case 4A in Fig. 6 – left-hand side), the effect is large, reducing the final temperature from 105 °C (case 2B in Fig. 2 – right hand side) to 65 °C (case 4A in Fig. 7). On the contrary, when the pre-cooling is applied to the first 100 s, the effect is not sufficient to decrease the temperature below the threshold and it is necessary to extend the pre-cooling to the first 170 s (case 4B in Fig. 6 – left-hand side) to achieve the target by a small margin (case 4B in Fig. 7). The energy savings in cases 4A and 4B are 19.3% and 40% respectively compared to case 1D.

It must be highlighted that for this specific pressure profile of the incoming gas, the larger mass flow rates occur in the second half of the filling as described in Fig. 5. Therefore also in this case, given the same pressure profile, the maximum saving occurs when the cooling is used during the time of the smaller mass flow rate (case 4B). Moreover with smaller mass flow rate, the application of the cooling is required for a shorter time than in the cases with higher mass flow rate.

As depicted in Fig. 6 (right-hand side) for cases 4C and 4D, a two-step pressure rise with decreasing rise rate with pre-cooling have been selected. As shown in Fig. 2 for case 2A, without pre-cooling the gas temperature exceeds the 85 °C within the first 60 s therefore it was necessary to apply the pre-cooling at an earlier stage of the filling, starting at 40 s for the last 160 s of the process in case 4C (Fig. 6 left-hand side). Pre-cooling the gas to −40 °C for the first 100 s was also sufficient for the purpose as shown in Fig. 7 for case 4D.

In case 4C and case 4D, the energy savings are 42.5% and 17.3% compared to case 1D, providing a confirmation that cooling the gas during the time of smaller mass flow filling rate (and smaller pressure rise rate) is more convenient (case 4C).

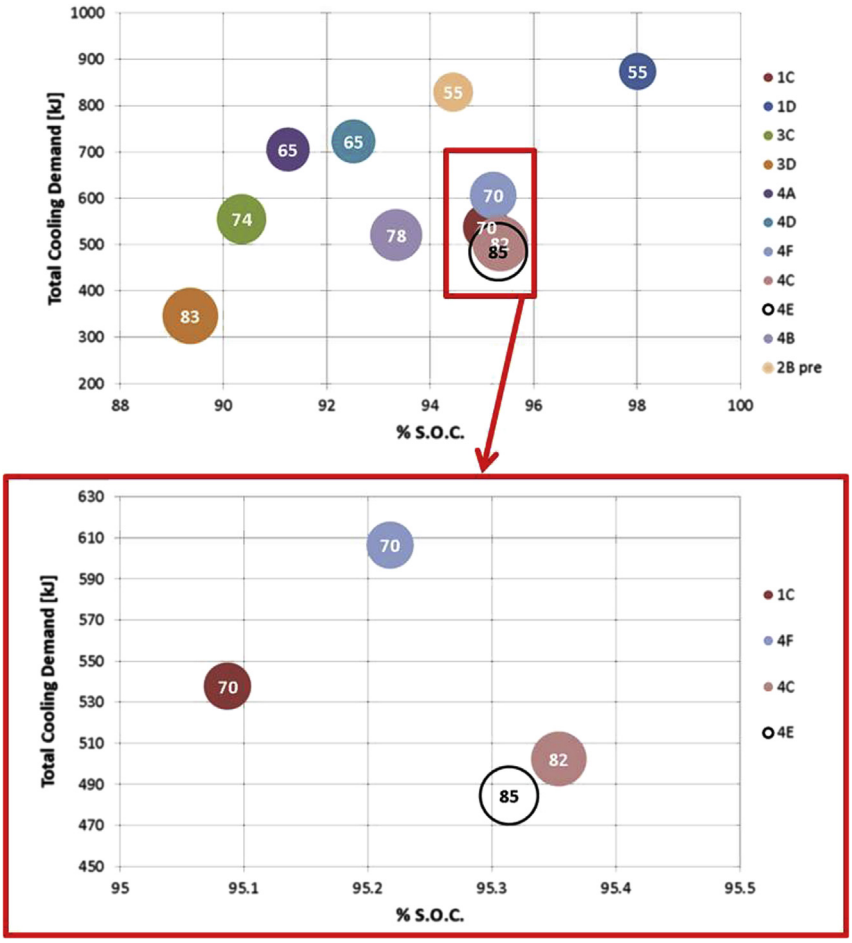

Fig. 9 – Total cooling demand versus SOC. The maximum gas temperature in the tank is indicated inside the circles.

Similar pre-cooling strategies are applied to a pressure profile with a multiple step-wise behaviour for cases 4E and 4F as described in Fig. 8 (left-hand side). The same pressure profile without pre-cooling has been applied in case 2C where the temperature goes beyond the limit at 60 s as depicted in Fig. 2. Therefore also in case 4E, the gas has been pre-cooled for the last 150 s and the final temperature has been decreased from 95 °C (case 2C – Fig. 2) to about 72 °C (case 4E – Fig. 8). Nevertheless the maximum temperature of 85 °C in Case 4E occurs at 20 s.

In case 4F, the pre-cooling is applied for the first 100 s and the final temperature is decreased to 70 °C compared to 95 °C for the non pre-cooled case 2C. The energy savings for case 4E and case 4F are 44.5% and 30% compared to case 1D. The largest saving occurs when the pre-cooling is employed during the time with lower mass flow rate (case 4E) although in this configuration the maximum temperature is higher than in case 4F by about 14 °C.

Final remarks

In Fig. 9, the total cooling demand, SOC and the maximum temperature are plotted in the same graph. In the circle the maximum temperature is provided for each case. Only the cases within the maximum allowed temperature are included in the graph. Case 2A_pre and case 2C_pre have not been included in the figure because they are overlapping with case 1D, having almost the same SOC (~98%) and total cooling energy demand (~880 kJ). The ideal region of the figure is in the lower right corner of the figure where at a high SOC corresponds a low cooling demand. On the other hand the worse region would be on the top left corner of the graph. None of the strategies that have been investigated in this study are in the ideal region or in the worse region. All the cases are placed almost linearly along a direction from the bottom left corner towards the top right corner that goes from case 3D (low SOC and low cooling demand with linear increase of pressure and pre-cooling in the last 100 s) to case 1D (high SOC and high cooling demand with linear pressure increase and pre-cooling to −40 °C for the whole duration of the process).

In Fig. 9, many different filling strategies achieve the temperature target with very different level of SOC and cooling demand. A SOC between 90% and 100% is considered typical [26]. In the appendix B of the SAE J2601 [3], the lower bounds for the SOC of vehicle fuel systems with capacity 1–7 kg with 2 MPa initial pressure go from 84% to 91% depending on the ambient temperature.

It is relevant to identify the ranges of the 3 key-parameters in all the cases where the maximum temperature is below the threshold during the whole duration of the filling. For the

maximum temperature, the range goes from 55 °C to 85 °C, for the theoretical cooling demand from 346 kJ to 882 kJ, and for the SOC from 89% to 98%. The maximum cooling energy saving occurs in case 3D where the required energy is 60% less compared to the case 1D, although the maximum temperature is 83 °C and the SOC is 89.3% and both values are at the edge of the acceptable ranges. A significant advantage occurs also for the theoretical maximum cooling power that is about 5 kW for case 3D and 10 kW for the case 1D according to equation (1). The worst cases for the maximum cooling power (~18 kW) are the case 2C_pre and case 4F where the pre-cooling is applied at the time of maximum mass flow rate among all the considered cases. That time is clearly placed in the first 20 s for case 2C, as shown in Fig. 5, which is the case without pre-cooling with the same pressure profile of the case 2C_pre and case 4F with pre-cooling. Higher peaks of mass flow rate require higher cooling power.

Conclusions

A CFD model was applied to investigate the effect of filling strategies on 3 key-parameters: the maximum temperature, the state of charge (SOC) and the theoretical cooling energy demand. The accuracy of the CFD model in the relevant conditions had been assessed in previous papers by the same group of authors. The gas temperature inside the tank cannot be larger than 85 °C in order to prevent changes in the mechanical properties of the material. Four strategies were considered to achieve that target. In the first strategy, the pre-cooling was applied for the whole duration of the process to an almost linear increasing pressure of the incoming gas. Pre-cooling to −40 °C (case 1D) and −20 °C achieved the temperature target for the gas inside the vessel while pre-cooling to 0 °C and no pre-cooling failed. In the second strategy, different step-wise pressure profiles were adopted with no pre-cooling and that approach was completely unsuccessful. Only with pre-cooling, the target temperature was achieved with the different step-wise pressure profiles but the energy saving was non-existing or minimal (5%) compared to case 1D. In the third strategy, step-wise temperature profiles with a linear increase of pressure were considered. Finally a step-wise function both for the pressure rise and for the temperature profile was selected. In the third and fourth approach pre-cooling (to −40 °C) was not applied for the whole duration of the filling but for a limited time, from 50% to 75% of the filling time.

The main findings related to the selected tank and selected boundary/initial conditions can be summarized as follows:

- Different filling strategies can be successfully implemented and they have significantly different effects on the SOC, maximum temperature and cooling demand energy.
- Pre-cooling is necessary to keep the gas temperature within the threshold for all considered pressure profiles.
- Pre-cooling to −40 °C is not necessary for the whole duration of the filling and pre-cooling for a fraction of the time can be sufficient to achieve the temperature target.
- Partial time pre-cooling to −40 °C can produce significant savings in term of total cooling energy compared to the cases with pre-cooling over the whole duration of the process.
- The maximum saving (~60%) is achieved for the case with an almost linear pressure rise and pre-cooling in the second half of the filling.
- Pre-cooling the gas in the stages with smaller pressure rise rate and therefore smaller mass filling rate is the more convenient approach from the point of view of the total cooling energy and the maximum cooling power. However that occurs at the expense of a higher maximum temperature and of a lower SOC.
- Precooling the gas in the stages with higher pressure rise rate (and therefore higher mass filling rate) requires larger cooling energy, higher cooling power peaks and the use of pre-cooling for longer times.

Acknowledgements

This work has been carried out within the multi-year program of the European Commission's Joint Research Centre (Institute for Energy and Transport) under the auspices of the SAFHYR project (Safety Aspects of Hydrogen Technologies Studied by Modelling and Sensor Tools). Special thanks are due to Marc Steen, Pietro Moretto, Beatriz Acosta-Iborra, Rafael Ortiz-Cebolla, and Nerea DeMiguel-Echevarria for the useful discussions on the topic.

REFERENCES

[1] Commission regulation (EU) no 406/2010 of 26 April 2010 implementing regulation (EC) no 79/2009 on type-approval of hydrogen-powered motor vehicles. Off J Eur Union 18.05.2010;L 122:1e107.
[2] SAE J2579. Technical information report for fuel system in fuel cells and other hydrogen vehicles. revised SAE Int March 2013.
[3] SAE J2601. Fueling protocols for light duty gaseous hydrogen Surface vehicles. SAE Int.
[4] ECE/TRANS/WP.29/2013/41. Proposal for a global technical regulation on hydrogen and fuel cell vehicles.
[5] International Standard Organization. Gaseous hydrogen and hydrogen blends land vehicle fuel tanks. ISO/TS 15869. 2009.
[6] Ortiz Cebolla R, Acosta B, Moretto P, Frischauf N, Harskamp F, Bonato C, et al. Hydrogen tank first filling experiments at the JRC-IET GasTeF facility. Int J Hydrogen Energy 2014;39(11):6261–7.
[7] Galassi MC, Baraldi D, Acosta Iborra B, Moretto P. CFD analysis of fast filling scenarios for 70 MPa hydrogen type IV tanks. Int J Hydrogen Energy 2012;37(8):6886–92.
[8] Melideo D, Baraldi D, Galassi MC, Ortiz Cebolla R, Acosta Iborra B, Moretto P. CFD model performance benchmark of fast filling simulations of hydrogen tanks with pre-cooling. Int J Hydrogen Energy 2014;39(9):4389–95.
[9] Galassi MC, Papanikolaou E, Heitsch M, Baraldi D, Iborra BA, Moretto P. Assessment of CFD models for hydrogen fast filling simulations. Int J Hydrogen Energy 2013;39(11):6252–60.

[10] Heitsch M, Baraldi D, Moretto P. Numerical investigations on the fast filling of hydrogen tanks. Int J Hydrogen Energy February 2011;36(3):2606–12.
[11] Dicken CJB, Merida W. Modeling the transient temperature distribution within a hydrogen cylinder during refueling. Numer Heat Transf Part A Appl 2007;53:685–708.
[12] Kim SC, Lee SH, Yoon KB. Thermal characteristics during hydrogen fueling process of type IV cylinder. Int J Hydrogen Energy 2010;35:6830–5.
[13] Suryan A, Kim HD, Setoguchi T. Three dimensional numerical computations on the fast filling of a hydrogen tank under different conditions. Int J Hydrogen Energy 2012;37:7600–11.
[14] Wang G, Zhou J, Hu S, Dong S, Wei P. Investigations of filling mass with the dependence of heat transfer during fast filling of hydrogen cylinders. Int J Hydrogen Energy 2014;39(9):4380–8.
[15] Takagi Y, Sugie N, Takeda K, Okano Y, Eguchi T, Hirota K. Numerical investigation of the thermal behaviour in a hydrogen tank during fast filling process. In: Proceedings of ASME/JSME 2011 8th thermal engineering joint conference [March 13–17, 2011, Honolulu, Hawaii, USA] AJTEC2011-44270. p. T10037-T10037-6.
[16] Ranong CN, Maus S, Hapke J, Fieg G, Wenger D. Approach for the determination of heat transfer coefficients for filling processes of pressure vessels with compressed gaseous media. Heat Transf Eng 2011;32(2):127–32.
[17] Li Q, Zhou J, Chang Q, Xing W. Effects of geometry and inconstant mass flow rate on temperatures within a pressurized hydrogen cylinder during refueling. Int J Hydrogen Energy 2012;37(7):6043–52.
[18] Zhao L, Liu Y, Yang J, Zhao Y, Zheng J, Bie H, et al. Numerical simulation of temperature rise within hydrogen vehicle cylinder during refueling. Int J Hydrogen Energy 2010;35:8092–100.
[19] Zhao Y, Liu G, Liu Y, Zheng J, Chen Y, Zhao L, et al. Numerical study on fast filling of 70 MPa type III cylinder for hydrogen vehicle. Int J Hydrogen Energy 2012;37:17517–22.
[20] ANSYS CFX. User's guide. Release 14.1. ANSYS Inc; 2013.
[21] Redlich O, Kwong JNS. On the thermodynamics of solutions: V. An equation of state: fugacity of gaseous solutions. Chem Rev 1949;44:233–44.
[22] Ouellette P, Hill PG. Turbulent transient gas injections. J Fluids Eng 2000;122:743–53.
[23] Pope SB. An explanation of the turbulent round-jet/plane-jet abnormality. Technical Note AIAA J 1978;16:279.
[24] Magi V, Iyer V, Abraham J. The k-e model and computed spreading in round and plane jets. Numer Heat Transf J 2001;40:317–34.
[25] Hirotani R, Tomioka J, Maeda Y, Mitsuishi H, Watanabe S. Thermal behavior in hydrogen storage tank for fuel cell vehicle on fast filling. In: World Hydrogen Energy Conference. Lyon, France; June 2006. p. 1–10.
[26] Schneider J, Sutherland I, Klugmann J, Hill HJ, Immel R, Cairns J, et al. The implementation of SAE TIR J2601: hydrogen fueling protocol guideline for demonstration projects. In: SAE World Conference; 2010.